Phase Equilibrium Relations and Structural Transition in the 1,1,1,2-Tetrafluoroethane Hydrate System

Yoshito Katsuta, Sumihiro Suzuki, Yuuki Matsumoto, Shunsuke Hashimoto†,

Takeshi Sugahara, and Kazunari Ohgaki*

Division of Chemical Engineering, Department of Materials Engineering Science, Graduate School of Engineering Science, Osaka University, 1-3 Machikaneyama, Toyonaka, Osaka 560-8531, Japan

ABSTRACT: The three-phase (hydrate, aqueous, and HFC-134a-rich liquid phases) equilibrium relations of the 1,1,1,2-tetrafluoroethane (HFC-134a) + water binary system were measured in a pressure range up to 293 MPa. The HFC-134a hydrate has a structural phase transition point from structure-II to structure-I at (65±1) MPa and (282.2±0.1) K, where the slope of the three-phase equilibrium curve is drastically changed. The Raman spectra of the HFC-134a molecule in the structure-I HFC-134a hydrate phase indicate that HFC-134a molecule occupies only large cage of structure-I at a pressure up to 293 MPa.

Keyword: Gas hydrate, Phase equilibria, Structural phase transition, Raman spectroscopy

INTRODUCTION

Gas hydrate is composed of guest species and hydrogen-bonded cages of the water molecules. There are two hydrate structures of structure-I (space group, *Pm*3*n* (s-I)) and structure-II (space group, *Fd*3*m* (s-II)). The unit cell of s-I hydrate is composed of two small cages (pentagonal dodecahedron (5^{12}, S-cage)) and six large cages (tetrakaidecahedron ($5^{12}6^2$, M-cages)), and that of s-II hydrate is composed of sixteen S-cages and eight large cages (hexakaidecahedron ($5^{12}6^4$, L-cage)).[1] The hydrate structure mainly depends on the size and shape of guest species in addition to temperatures and pressures. For example, SF_6 molecule is enclathrated into only L-cages of s-II at pressures below 33 MPa.[2] Above 33 MPa, SF_6 molecule is enclathrated into M-cage of s-I, so SF_6 hydrate system has the structural phase transition point at (33 MPa, 288 K).

Recently, many researchers have studied gas hydrates to be utilized as a heat medium. Hydrofluorocarbons (HFCs) have large enthalpy of vaporization, so HFCs are used as refrigerants. Among them, HFC-134a is more effective and it has been used as air-conditioner. Moreover, the dissociation enthalpy of HFC-134a hydrate is much larger than vaporization enthalpy of HFC-134a.[3,4] Therefore, the usage of the HFC-134a hydrate is implied to result in more cooling efficiency. For the HFC-134a hydrate system, the three-phase equilibrium curves of (H+L_1+G), (H+L_2+G), and (L_1+L_2+G) and the quadruple point of Q_2 (H+L_1+L_2+G) in the temperature range of (273.95 to 294.19) K and the pressure range of (0.062 to 9.68) MPa has already been reported.[3,5] However, there are only three equilibrium data at pressures higher than that of Q_2. The symbols of H, L_1, L_2, and G represent hydrate, aqueous, HFC-134a-rich liquid, and gas phases, respectively.

In the present study, we have investigated the high-pressure phase equilibria of HFC-134a hydrate based on the following data: (i) the three-phase (H+L_1+L_2) equilibrium curve of the HFC-134a hydrate system in a temperature range of (282.2 to 301.6) K and a pressure range of

(10.6 to 293) MPa (ii) the Raman spectra of the intramolecular and intermolecular vibrations of HFC-134a and host water molecules in the single crystal of HFC-134a hydrate (iii) the powder X-ray diffraction (PXRD) analysis of HFC-134a hydrate.

EXPERIMENTAL SECTION

For the simultaneous measurements of the phase equilibrium relation and in situ Raman spectra, we used the custom-made high-pressure optical cell. The details of the high-pressure optical cell are given elsewhere.[2] Two types of pressure gauges depending on experimental pressures were used. Up to 60 MPa, a pressure gauge (Valcom, model: VPRT) calibrated by a Ruska quartz Bourdon tube gauge was used with an estimated maximum uncertainty of 0.15 MPa. Over 60 MPa, a pressure transducer (NMB, model: STD-5000K) and digital peak holder (NMB, model: CSD-819) were used with an estimated maximum uncertainty of 2 MPa. The equilibrium temperature was measured within a reproducibility of 0.02 K by a thermistor probe (Takara, model: D-632).

In advance, the high-pressure optical cell was evacuated. After that, HFC-134a was introduced into the cell. The cell was immersed in a thermocontrolled water bath to control the temperature. The distilled and degassed water was introduced into the cell and pressurized by supplying distilled water by use of a high-pressure pump. A ruby ball was introduced into the cell in advance to agitate the contents inside the cell. The cell was subcooled and agitated to generate hydrates. The phase behavior was observed directly by use of charge-coupled device (CCD) through the sapphire window. After the confirmation of hydrate formation, the temperature was controlled to establish the three-phase ($H+L_1+L_2$) coexistence state. When the pressure reached a plateau and three-phase coexistence was directly observed, the pressure and temperature were determined as the three-phase equilibrium pressure and temperature, respectively. Once the

hydrate sample was taken from the cell at liquid nitrogen temperature, the sample was grained in the mortar immersed in liquid nitrogen. The PXRD pattern was measured by use of a diffractometer (Rigaku, model: Ultima IV) with a Rigaku D/teX ultra high-speed position sensitive detector and Cu Kα X-ray (40 kV, 50 mA). The PXRD measurements were performed at 153 K and atmospheric pressure in the stepscan mode with scan rate of 4 deg/min and step size of 0.02°. The PXRD pattern indexing and cell refinement were obtained by use of the Chekcell[6] and PowderX[7] programs and the initial lattice parameters[1] for the refinement.

The single crystal of HFC-134a hydrate was prepared on the stability boundary. The crystal was analyzed through a sapphire window by use of a laser Raman microprobe spectrometer with a multichannel CCD detector (Jobin Yvon, model: Ramanor T64000). The light source for excitation was argon ion laser whose wavelength, power level, and spot diameter were 514.5 nm, 100 mW, and 2 μm, respectively. The laser beam from the object lens was irradiated to every phase through the upper sapphire window. The backscatter of the opposite direction was taken in through the lens. The spectral resolution was approximately 0.7 cm^{-1}.

The materials used in the present study were summarized in Table 1. Both were used without further purification.

RESULTS AND DISCUSSION

The phase equilibria for the HFC-134a+water binary system are shown in Figure 1 and three-phase ($H+L_1+L_2$) equilibrium data are summarized in Table 2. The slope (dp/dT) of three-phase ($H_{II}+L_1+L_2$) equilibrium curve originated from the quadruple point Q_2 (0.416 MPa, 283.19 K)[3] is negative, while the dp/dT changes positive at (65±1) MPa and (282.2±0.1) K. The slope change results from the structural phase transition in the HFC-134a hydrate phase. Similar behavior of equilibrium curves has been observed in the THF+water (200 MPa, 268 K)[8] and the

propane+water (145 MPa, 272.95 K)[9]. According to Clapeyron equation, the negative slope ($dp/dT < 0$) means that the molar volume change of hydrate is larger than that of reactant (mixture of the saturated HFC-134a liquid and water). The rough estimation of the molar volume change before and after the HFC-134a hydrate formation supports the negative slope, where the molar volumes of liquefied HFC-134a, water, and s-II HFC-134a hydrate are estimated by use of Soave-Redlich-Kwong equation of state,[10] Saul-Wagner equation,[11] and the lattice constant of 1.73 nm, respectively.

The PXRD pattern for the HFC-134a hydrate prepared at 70 MPa indicates the existence of the s-I HFC-134a hydrate. Moreover, the lattice parameter a = (1.204±0.002) nm is similar to the literature value.[1] From the result of PXRD and phase equilibrium measurement, we have concluded that the HFC-134a hydrate structure changes from s-II to s-I.

The Raman spectra in the HFC-134a hydrate phase were in-situ measured along the thermodynamic stability boundary. The Raman shift ($\Delta\nu$) of the C–C symmetric stretching vibration of HFC-134a in the hydrate phase under the three-phase equilibrium condition is shown in Figure 2. The Raman shifts and peak width at 88 MPa are clearly different from those at 20 MPa. The pressure dependences of the Raman shifts corresponding to the C–C and C–H stretching vibration modes are shown in Figure 3 and summarized in Table 3. Both Raman shifts change on each side of the structural phase transition point at 65 MPa. The single Raman peaks of the C–C symmetric stretching vibration are in good agreement with the reported ones in L-cage (841 cm^{-1}) and M-cage (847 cm^{-1}) of the s-II and s-I difluoromethane+HFC-134a mixed-gas hydrates, respectively.[12] At pressures above 65 MPa, the Raman shifts are almost constant and remain single in a pressure range up to 290 MPa. As reported previously,[2,13–17] the Raman shifts corresponding to the intramolecular vibration of guest species in M-cage or L-cage are independent of a pressure up to 500 MPa. In the case of the HFC-134a hydrate, the trend is

similar. Single Raman peak in each vibration modes of HFC-134a molecule indicates no HFC-134a molecule occupies S-cage.

In addition to the intramolecular vibration modes of guest molecules, in hydrate phase, the broad peak corresponding to the intermolecular O–O vibration (lattice mode) between H_2O molecules of hydrate cages was detected around 205 cm^{-1}. Table 3 includes the results of the lattice mode. The Raman spectrum of the lattice mode depends on the hydrate structures, the pressure, and temperature conditions. Especially on the thermodynamic stability boundary of hydrates, the pressure dependences of the lattice mode are peculiar to the hydrate crystal structures for the s-I and s-II.[13–20] There are two tendencies in the s-I hydrate systems; one is a strong pressure dependence of type A (CH_4,[13] CO_2,[18] and Xe [19]), and the other is a very weak pressure dependence of type B (C_2H_4,[14] C_2H_6,[15] cyclopropane,[16] and CF_4[17]). The stronger pressure-dependence of type A would indicate a higher shrinkage of the hydrogen-bonded cage or the larger free volume for the guest molecule. On the other hand, the guest molecule having a large van der Waals diameter generates the type B hydrate crystal. At 20 MPa, the Raman shift of the lattice mode in s-II HFC-134a hydrate agrees with that of other s-II hydrates.[2,21] At pressures from 88 MPa to 290 MPa, the Raman shift coincides with the type B of the s-I hydrates.

CONCLUSION

The phase equilibria of the HFC-134a+water binary system at a pressure up to 293 MPa have been measured. Based on the discontinuity of dp/dT on the stability boundary and PXRD analysis, HFC-134a hydrate has the structural phase transition point at (65±1) MPa, (282.2±0.1) K. The hydrate structure changes from s-II at pressures below 65 MPa to s-I above 65 MPa. HFC-134a molecule is enclathrated into only M-cage even at 293 MPa.

Figure captions

Figure 1. Three-phase equilibrium relation for the HFC-134a+water binary system. Open circles, $H_{II}+L_1+L_2$ (present study); open squares, $H_I+L_1+L_2$ (present study); closed triangle, structural transition point (present study); closed rhombuses, $H_{II}+L_1+G$;[5] open rhombuses, $H_{II}+L_1+G$;[3] open inverse triangles, $H_{II}+L_2+G$;[3] open triangles, L_1+L_2+G;[3] closed circles, $H_{II}+L_1+L_2$;[3] closed square, quadruple point $Q_2(H_{II}+L_1+L_2+G)$[3]. The symbols H_I, H_{II}, L_1, L_2, and G represent structure-I hydrate, structure-II hydrate, aqueous, HFC-134a-rich liquid, and gas phases.

Figure 2. Raman spectra of the intramolecular C–C stretching vibration in the HFC-134a hydrate. (a) s-II HFC-134a hydrate at 20 MPa and 283.06 K, (b) s-I HFC-134a hydrate at 88 MPa and 284.96 K.

Figure 3. Pressure dependence of Raman shifts corresponding to the (a) C–C and (b) C–H symmetric stretching vibrations in the HFC-134a hydrate phase along three-phase equilibrium curves of $H_{II}+L_1+L_2$ (below 65 MPa) and $H_I+L_1+L_2$ (above 65 MPa). The open and closed keys stand for the results in the present study and ref 12, respectively.

Table 1. Information on the Chemicals Used in the Present Study.

Chemical Name	Source	Mole Fraction Purity
1,1,1,2-tetrafluoroethane	Daikin Ind., Ltd.	> 0.996
water	Wako Pure Chemicals Ind., Ltd.	> 0.9999

Table 2. Three-Phase (Hydrate, Aqueous, and HFC-134a-rich Liquid Phases) Equilibrium Data (Temperature T, Pressure p) for the HFC-134a+Water System.[a] The Structural Phase Transition Point is Located at (282.2±0.1) K and (65±1) MPa.

T / K	p / MPa
283.12	10.63
283.14	18.32
283.04	20.02
282.93	30.03
282.82	34.75
282.77	42.04
282.63	49.73
282.53	54.77
282.27	65
282.79	70
283.97	81
284.70	87
286.37	100
288.02	116
290.28	141
291.69	156
292.78	171
294.07	187
297.51	229
298.69	245
299.96	266
301.62	293

[a] Standard uncertainties u are $u(p) = 0.15$ MPa at $p < 60$ MPa and $u(p) = 2$ MPa at $p > 60$ MPa, $u(T) = 0.02$ K.

Table 3. Pressure Effect (Pressure p, Raman Shift $\Delta\nu$) on the Intermolecular O–O Stretching Vibration and the Intramolecular C–C and C–H Stretching Vibrations in the HFC-134a Hydrate Phase. [a]

p / MPa	0.17 [b]	20	88	173	290
Stretching Vibration Mode			$\Delta\nu$ / cm^{-1}		
O–O	-	210	204	203	205
C–C Symmetric	841	841	846	845	847
C–H Symmetric	2977	2979	2987	2988	2986
C–H Asymmetric	-	2993	3022	3025	3024

[a] Standard uncertainties u are $u(p)$= 2 MPa, $u(\Delta\nu)$= 1 cm^{-1}.

[b] From Ref 12

AUTHOR INFORMATION

Corresponding Author

* Tel.&Fax.: +81-6-6850-6293. E-mail: sugahara@cheng.es.osaka-u.ac.jp

Present Addresses

†Dr. S. Hashimoto, Thermal Management Lab. Toyota Central R&D Labs., Inc., 41-1 Yokomichi, Nagakute, Aichi 480-1192, Japan

ACKNOWLEDGMENT

We acknowledge the material supports from the Daikin Industries, Ltd. We also acknowledge the scientific supports from the "Gas-Hydrate Analyzing System (GHAS)" of the Division of Chemical Engineering, Graduate School of Engineering Science, Osaka University (for the Raman analyses) and Rigaku Corporation (for the PXRD measurement at low temperatures). We thank Dr. H. Sato (Osaka University), Mr. T. Kido (Daikin Industries), and Mr. K. Nagao (Rigaku Corporation) for the valuable discussion and suggestions.

REFERENCES

(1) Sloan, E.D.; Koh, C.A. *Clathrate Hydrates of Natural Gases*, 3rd ed.; CRC Press, Taylor & Francis Group: Boca Raton, FL, **2008**.

(2) Sugahara, K.; Yoshida, M.; Sugahara, T.; Ohgaki, K. Thermodynamic and Raman Spectroscopic Studies on Pressure-Induced Structural Transition of SF_6 Hydrate. *J. Chem. Eng. Data* **2006**, *51*, 301–304.

(3) Hashimoto, S.; Makino, T.; Inoue, Y.; Ohgaki, K. Three-Phase Equilibrium Relations and Hydrate Dissociation Enthalpies for Hydrofluorocarbon Hydrate Systems: HFC-134a, -125, and -143a Hydrates. *J. Chem. Eng. Data* **2010**, *55*, 4951–4955.

(4) Ogawa, T.; Ito, T.; Watanabe, K.; Tahara, K.; Hiraoka, R.; Ochiai, J.; Ohmura, R.; Mori, Y. Development of a Novel Hydrate-Based Refrigeration System: A Preliminary Overview. *Appl. Therm. Eng.* **2006**, *26*, 2157–2167.

(5) Liang, D.; Guo, K.; Wang, R.; Fan, S. Hydrate Equilibrium Data of 1,1,1,2-tetrafluoroethane (HFC-134a), 1,1-dichloro-1-fluoroethane (HCFC-141b) and 1,1-difluoroethane (HFC-152a). *Fluid Phase Equilib.* **2001**, *187–188*, 61–70.

(6) *Chekcell*; http://www.ccp14.ac.uk. Chekcell developed by Laugier, L.; Bochu, B. Laboratoire des Materiaux et du Genie Physique, Ecole Superieure de Physique de Grenoble: Grenoble, France (accessed April 28, 2011).

(7) Dong, C. PowderX: Windows-95-based Program for Powder X-ray Diffraction Data Processing. *J. Appl. Crystallogr.* **1999**, *32*, 838.

(8) Manakov, A. Y.; Goryainov, S.V.; Kurnosov, A.V.; Likhacheva, A.Y.; Dyadin, Y.A.; Larionov, E.G. Clathrate Nature of the High-Pressure Tetrahydrofuran Hydrate Phase and Some New Data on the Phase Diagram of the Tetrahydrofuran-Water System at Pressures. *J. Phys. Chem. B* **2003**, *107*, 7861–7866.

(9) Dyadin, Y.A.; Larionov, E.G.; Aladko, E.Ya.; Zhurko, F.V. Clathrate Formation in Propane–Water and Methane–Propane–Water Systems under Pressures of up to 15 kbar. *Dokl. Phys. Chem.* **2001**, *376*, 23–26.

(10) Soave, G. Equilibrium Constants from a Modified Redlich-Kwong Equation of State. *Chem. Eng. Sci.* **1972**, *27*, 1197–1203.

(11) Saul, A.; Wagner, W. A Fundamental Equation for Water Covering the Range from the Melting Line to 1273 K at Pressures up to 25000 MPa. *J. Phys. Chem. Data* **1989**, *18*, 1537–1564.

(12) Miyauchi, H.; Yasuda, K.; Matsumoto, Y.; Hashimoto, S.; Sugahara, T.; Ohgaki, K. Isothermal Phase Equilibria for the (HFC-32+HFC-134a) Mixed-gas Hydrate System. *J. Chem. Thermodyn*. **2012**, *47*, 1–5.

(13) Nakano, S.; Moritoki, M.; Ohgaki, K. High-Pressure Phase Equilibrium and Raman Microprobe Spectroscopic Studies on the Methane Hydrate System. *J. Chem. Eng. Data* **1999**, *44*, 254–257.

(14) Sugahara, T.; Morita, K.; Ohgaki, K. Stability Boundaries and Small Hydrate-Cage Occupancy of Ethylene Hydrate System. *Chem. Eng. Sci*. **2000**, *55*, 6015-6020.

(15) Morita, K.; Nakano, S.; Ohgaki, K. Structure and Stability of Ethane Hydrate Crystal. *Fluid Phase Equilib*. **2000**, *169*, 167–175.

(16) Suzuki, M.; Tanaka, Y.; Sugahara, T.; Ohgaki, K. Pressure Dependence of Small-Cage Occupancy in the Cyclopropane Hydrate System. *Chem. Eng. Sci*. **2001**, *56*, 2063–2067.

(17) Sugahara, K.; Yoshida, M.; Sugahara, T.; Ohgaki, K. High-Pressure Phase Behavior and Cage Occupancy for the CF_4 Hydrate System. *J. Chem. Eng. Data* **2004**, *49*, 326–329.

(18) Nakano, S.; Moritoki, M.; Ohgaki, K. High-Pressure Phase Equilibrium and Raman Microprobe Spectroscopic Studies on the CO_2 Hydrate System. *J*. *Chem*. *Eng*. *Data* **1998**, *43*, 807–810.

(19) Sugahara, K.; Sugahara, T.; Ohgaki, K. Thermodynamic and Raman Spectroscopic Studies of Xe and Kr Hydrates. *J*. *Chem*. *Eng*. *Data* **2005**, *50*, 274–277.

(20) Sugahara, K.; Kaneko, R.; Sasatani, A.; Sugahara, T.; Ohgaki, K. Thermodynamic and Raman Spectroscopic Studies of Ar Hydrate System. *Open Thermodyn*. *J*. **2005**, *50*, 274-277.

(21) Takasu, Y.; Iwai, K.; Nishio, I. Low Frequency Raman Profile of Type II Clathrate Hydrate of THF and Its Application for Phase Identification. *J*. *Phys*. *Soc*. **2003**, *5*, 1287-1291.

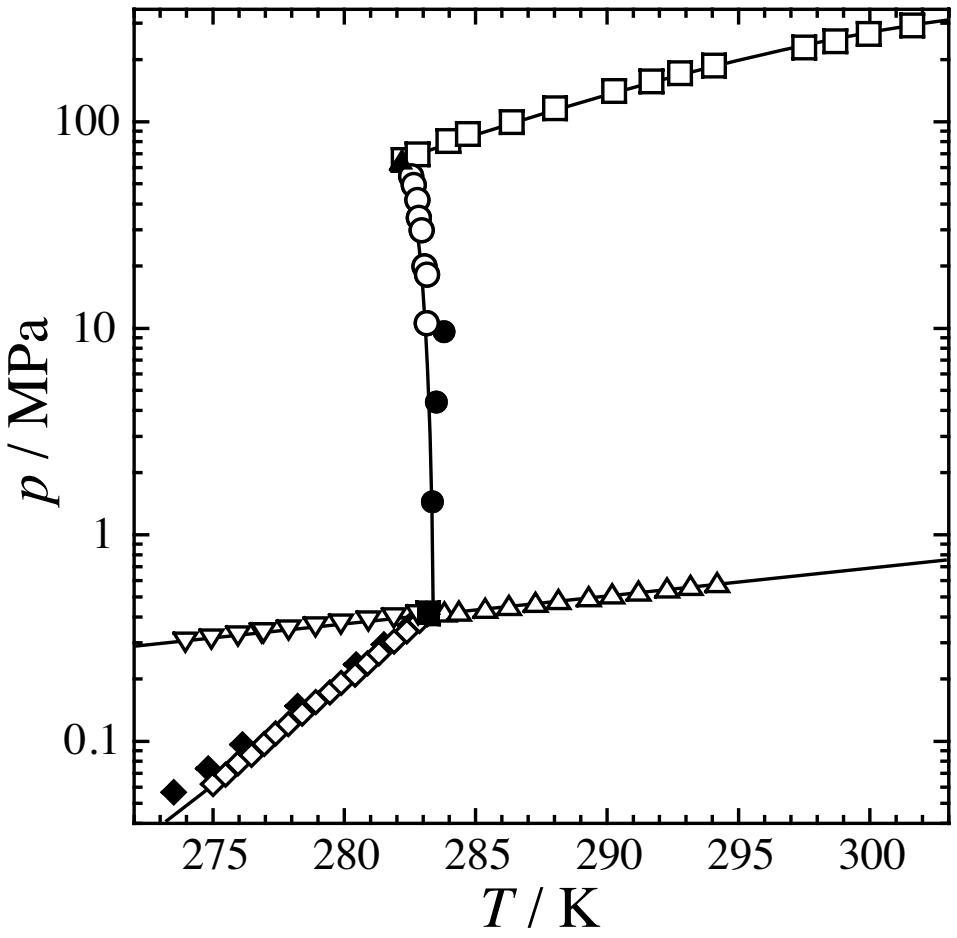

Figure 1. Three-phase equilibrium relation for the HFC-134a+water binary system. Open circles, $H_{II}+L_1+L_2$ (present study); open squares, $H_I+L_1+L_2$ (present study); closed triangle, structural transition point (present study); closed rhombuses, $H_{II}+L_1+G$;[5] open rhombuses, $H_{II}+L_1+G$;[3] open inverse triangles, $H_{II}+L_2+G$;[3] open triangles, L_1+L_2+G;[3] closed circles, $H_{II}+L_1+L_2$;[3] closed square, quadruple point $Q_2(H_{II}+L_1+L_2+G)$[3]. The symbols H_I, H_{II}, L_1, L_2, and G represent structure-I hydrate, structure-II hydrate, aqueous, HFC-134a-rich liquid, and gas phases.

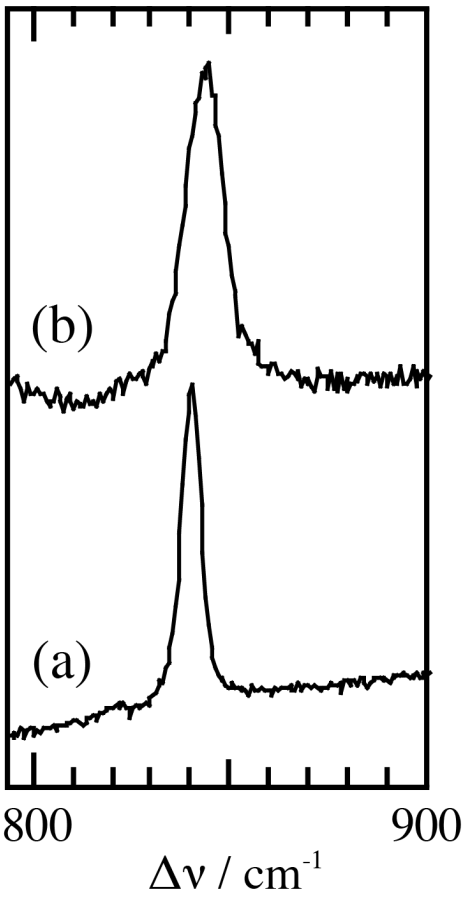

Figure 2. Raman spectra of the intramolecular C–C stretching vibration in the HFC-134a hydrate. (a) s-II HFC-134a hydrate at 20 MPa and 283.06 K, (b) s-I HFC-134a hydrate at 88 MPa and 284.96 K.

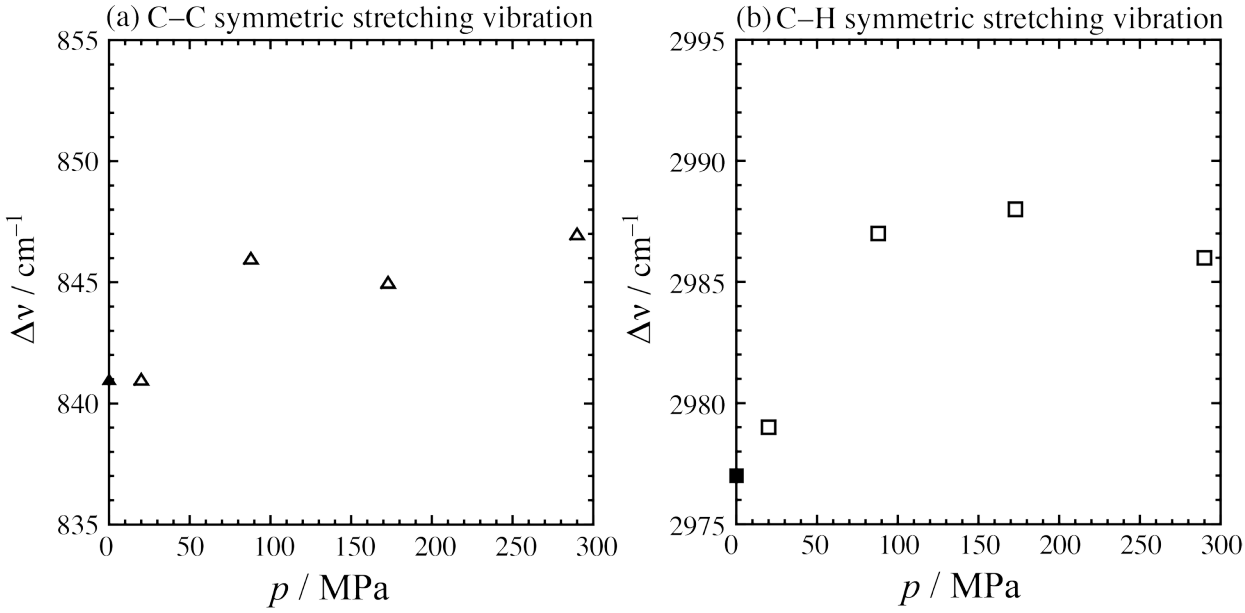

Figure 3. Pressure dependence of Raman shifts corresponding to the (a) C–C and (b) C–H symmetric stretching vibrations in the HFC-134a hydrate phase along three-phase equilibrium curve of H_{II}+L_1+L_2 (below 65 MPa) and H_I+L_1+L_2 (above 65 MPa). The open and closed keys stand for the results in the present study and ref 12, respectively.

TOC